SIMULATION OF SEMICONDUCTOR DEVICES AND PROCESSES Vol. 3
Edited by G. Baccarani, M. Rudan - Bologna (Italy) September 26-28, 1988 - Tecnoprint

NUMERICAL SIMULATION OF THE SPREADING RESISTANCE OF A BURIED RIDGE STRIPE SEMICONDUCTOR LASER

K. SOUISSI, E. CAQUOT*

Institut National de Recherche en Informatique et Automatique
BP 105, 78153 Le Chesnay CEDEX, FRANCE

* Centre National d'Etudes des Télécommunications
Laboratoire de Bagneux
196, Av. H. Ravéra, 92220 Bagneux, FRANCE

ABSTRACT

A 2D numerical simulation using Finite Element technique is presented to compute the spreading resistance of a semiconductor Buried Ridge Stripe laser. A simplified model of the electric conduction in the cladding layer of such laser is described. This highly non-linear model is solved in realistic laser geometry with use of quasi-Newton algorithm in order to compute the current flowing across the active region of the laser and the parasitic leakage current which can limited the laser performances.

1 - INTRODUCTION

Numerical simulations have been proved to be a very efficient way to optimize semiconductor devices and to understand their intrinsic behaviour. Near the well-known semiconductor transistors such as silicon MOSFET and GaAs MESFET, a wide class of semiconductor devices can be simulated as well by use of similar numerical techniques. The aim of this paper is to present the two-dimensional simulation of a particular semiconductor laser which is well-suited for high speed direct modulation : the Buried Ridge Stripe (BRS) laser[1][2][3][4]. This BRS laser presents, near its interesting intrinsic potential due the high photon density confined in the narrow buried active region, a quite versatile realization process. They are "planar" structures and the laser layers can be grown by various epitaxial techniques such as Liquid Phase Epitaxy, Metal-Organic Chemical Vapour Deposition or Molecular Beam Epitaxy. Unfortunately, the high intrinsic modulation and the low threshold current capabilities of such laser are often screened by parasitic leakage current outside the buried active region of the laser.

A simplified model of the electric conduction inside the upper or cladding layer of a BRS laser will be firstly described and will lead to a conventional Dirichlet problem with highly non-linear mixed boundary conditions. Part 3 details the two-dimensional numerical analysis of the resulting discrete problem when classic Finite Element technique is used to mesh the device. Some results are given in part 4 for a specific device and are compared with experimental results.

2 - MODEL OF ELECTRIC CONDUCTION OF A BRS LASER

The upper layer or cladding layer of a BRS laser (figure 1) is usually realized with a P-type InP or GaAs material (2 μm and doping level = 4.10^{17} cm^{-3}). In such a layer, considering the high current densities, a local electric neutrality is assumed. The main reason of current leakage outside the active region is the current flow across the P-type InP cladding layer and N-type InP buffer layer(this junction will be called in the paper the "homojunction"). The electric confinement is due to the fact that the junction between the cladding layer and the InGaAsP active region stripe (called "heterojunction") has a threshold voltage lower than the homojunction one. The current I versus potential u characteristics for these two junctions are experimentally measured on special test structures (figure 2). The dependence of I versus u can be well approximated by the well-known S hokley formula:

$$(eqn.\ 1) \qquad I = I_s \times \left(\exp\left(\frac{u}{n \times U_t} \right) - 1 \right)$$

where Ut = kT/q is the thermal voltage, q the electron charge, T the temperature, k the Boltzman constant, Is is the saturation current and n is the ideality factor of the junction.

This equation (1) can be applied as well for the local current density J,

$$(eqn.\ 2) \qquad J = J_s \times \left(\exp\left(\frac{u}{n \times U_t} \right) - 1 \right)$$

Parameter	Value	Unit
n_1	1	
$J_s{}^1$	10^{-16}	A/cm^{-2}
n_2	1.5	
$J_s{}^2$	$9\ 10^{-9}$	A/cm^{-2}
μ_p	80	$cm^{-2}V^{-1}s^{-1}$
p	5.10^{17}	cm^{-3}
e_0	0.2	µm
l_0	1.7	µm
e_1	1.5	µm
e_2	0.5	µm
l_2	8	µm
l_3	4	µm
θ	54	degrees
Z	250	µm

Table 1 : Numerical data of the physical parameters

This model, which is quite simple, has been found to be sufficient to understand the basic behaviour of the spreading resistance inside the cladding layer of BRS laser and to compute the leakage current in various structures.

3 - NUMERICAL ANALYSIS

This model leads to a non conventional problem with non-linear mixed boundary conditions. A detailed analysis of the mathematical properties of such a problem can be found elsewhere[5]. In this chapter, we shall describe the basic numerical tools which have been used to solve it.

1 - Discretization

In order to describe a real laser geometry, we have used the process modeller TITAN III-V[6]. After a description of the device with use of the elemental process steps, TITAN III-V uses an automatic triangular mesh generator, which can easily conform to any device geometry. It is based upon the Voronoi method[7]. Figure 3 shows the triangular mesh of the upper layer of the BRS laser in two dimensions: there are 2118 triangles, 1144 nodes.

Inside the cladding layer, the current will be assumed to be driven by the electrical field only (that means that no electron or hole diffusion occurs), because of the quite high doping level. Consequently, this layer can be assumed to be very similar to a metal and

$$(eqn.\ 3) \qquad J = \sigma E = -\sigma \nabla u$$

where J is the local current density, σ the conductivity, E the electrical field. At both homojunction and heterojunction, equation (3) holds and, consequently

$$(eqn.\ 4) \qquad -\sigma \frac{\partial u}{\partial n} = J_s \times \left(\exp\left(\frac{u}{n \times U_t} \right) - 1 \right)$$

where $\partial u/\partial n$ is the outward normal derivative of u.

In summary, the simplified electric model of the electrical conduction inside the cladding layer is:

$$(eqn.\ 5) \qquad \nabla(\epsilon \nabla u) = 0$$

inside the layer (Ω)

$$(eqn.\ 6) \qquad -\sigma \frac{\partial u}{\partial n} = J_s^1 \times \left(\exp\left(\frac{u}{n_1 \times U_t} \right) - 1 \right)$$

at the homojunction (Γ_1)

$$(eqn.\ 7) \qquad -\sigma \frac{\partial u}{\partial n} = J_s^2 \times \left(\exp\left(\frac{u}{n_2 \times U_t} \right) - 1 \right)$$

at the heterojunction (Γ_2)

The upper boundary conditions are classic

$$(eqn.\ 8) \qquad u = u_{app}$$

at the ohmic contacts (Γ_D)

$$(eqn.\ 9) \qquad \frac{\partial u}{\partial n} = 0$$

elsewhere (Γ_N)

The electric conductivity σ is given by the carrier mobility μ_p and doping level p by the conventional law

$$(eqn.\ 10) \qquad \sigma = q \times \mu_p \times p$$

The data used for the simulation work are summarized in table 1.

2 - Linearization methods

The discretization procedure presented in the previous chapter leads to the non-linear equation in which the unknowns are the values of the electrostatic potential at each node.

We will write the non-linear system to be solved as

$$(eqn.\ 11) \qquad F(u) = 0$$

The equation (11) may be solved by various ways; for example, using Newton's method[8], in this case we have

$$(eqn.\ 12) \qquad u^{k+1} = u^k - H^{-1} F(u^k)$$

where H is the jacobian of F.

The methods under discussion have the form

$$(eqn.\ 13) \qquad H(u^k)\delta u^k \equiv H_k \delta u^k = -F(u^k) \equiv -F_k$$

and

$$(eqn.\ 14) \qquad u^{k+1} = u^k + T_k \delta u^k$$

Here T_k is a suitably chosen diagonal matrix. If T_k is chosen to be the identity matrix, then (14) is the conventional Newton's method. If the method generates a sequence u^k such that u^k --> $u*$, then it is desirable that the norm of F_k monotonously approaches zero, when k increases, because this ensures that each iterate is an improvement over its predecessor. Unfortunately, Newton's method cannot guarantee, in this kind of problems, that

$$(eqn.\ 15) \qquad |F_{k+1}| < |F_k|$$

This is due essentially to the fact that the initial guess is not close to the solution. Newton's method can suffer from overshoot; that means that the Newton correction δu^k overestimates the length of the step which should have been taken.

In TITAN III-V, we have implemented a strategy to modify the Newton's method, so that the effects of overshoot are smoothed. This strategy limits each term of δu^k independently and it is called damping or clamping. In this method, the j^{th} diagonal entry in T_k is given by

$$T_k^j \qquad \begin{array}{ll} 1 & if \quad U_m \le u_j^k + \delta u_j^k \le U_M \\ \left(U_M - u_j^k\right) & if \quad u_j^k + \delta u_j^k > U_M \\ \left(U_m - u_j^k\right) & if \quad u_j^k + \delta u_j^k < U_m \end{array}$$

where U_m, U_M are the upper and lower bounds respectively of the function u(.). Estimates for the bounds is obtained from a maximum principle.

Remark 1 : This method is well accurate for any initial guess and avoid the phenomenon of overshoot and enhance the rate of convergence.

3 - Solution of the linear system

The system of the linear equations that occur in the solution process for discretized equation is solved by preconditioned conjugate gradient method [9].

Remark 2 : A remarkable time-saving can be achieved by avoiding to solve exactly the linear system.

4 - RESULTS, DISCUSSION

The model described in part 2 has been solved with use of the algorithms presented in part 3 for some BRS laser structures in order to identify the position of the leakage current across the P-type InP cladding layer and the N-type buffer layer homojunction. The simulated device is shown in figure 2 and the numerical data used during the simulation work are presented in Table 1 and are typical for this kind of laser. For this device, the ratio of the leakage current flowing through the device has been computed for various biases applied at the upper Schottky contact and results are given in Table 2.

1 - Equipotential plots

When applied voltage u_{app} increases, three regimes can be identified :

\- 1 / The first one corresponds to the region I of the current versus voltage characteristics of both homojunction and heterojunction ($u_{app} < V_2$). The current flowing across these boundaries is very small and Figure 4 shows the equipotential curves inside the cladding layer. The current begins to flow in this regime at the middle of the active layer for symmetry reasons. As the problem is in this case almost a linear Dirichlet problem, the number of Newton's iteration loops is quite small.

- 2 / The second one corresponds to the region II of figure 2 where current flows across the heterojunction only ($V_2 < u_{app} < V_1$). Note on Figure 5 the quasi-constant potential at the heterojunction which is imposed by the turn-on voltage of this junction. The problem is then highly non-linear because of the exponential boundary conditions and it is solved in less than 10 Newton's iteration loops.

- 3 / The third regime corresponds to the region III of figure 2. Current begins to flow through homojunction and the leakage current to grow ($u_{app} > V_1$). The equipotential curves (Figure 6) show that, in this particular device, the position where the leakage current is maximum lies at 2 μm from the edge of the active layer and not, as it could be assumed, very near of this edge. This distance can be easily explained by the fact that the electric potential is continuous and that the voltage drop $V_1 - V_2$ must be distributed along the homojunction contact. The problem is then more highly non-linear and 15 Newton's iteration loops are necessary to solve the problem with a accuracy of 10^{-5} with the L_∞ norm.

2 - Comparison with experimental results

The data reported in table 2 have been found to be in good agreement with experimental data obtained in our laboratory, considering the total current flowing through the laser diode. As it is quite difficult to measure a leakage current, the results obtained by this two-dimensional simulation have been used in order to deduce the complete dynamic distributed model and the results of the optical dynamic response of experimental lasers have been compared with the simulated response obtained by this model[10]. Agreement has been found pretty good.

Applied voltage (V)	Total current (mA)	Active current (mA)	Leakage current (mA)
0.8	0.35	0.331	1.7 10^{-2}
1.	20.88	16.8	4.08
1.2	85.82	52.73	33.05
1.4	167	87.85	79.12

Table 2 : Active and leakage current at various applied voltage

5 - CONCLUSION

In this paper, the simplified model of the electric conduction in the cladding layer of a BRS laser has been numerically solved with use of Finite Element techniques and modified Newton's algorithm. A user-oriented software based on the TITAN III-V package has been written and can be used by process engineers in order to optimize the BRS laser and to compare the various realization possibilities between them. These 2-D simulations have permitted to deduce an analytic distributed model of the laser, which is now used for optoelectronic circuit design. Further improvements will be achieved by solving the complete set of the fundamental semiconductor equations in the real geometry of the device, but a major difficulty in this case, is to find the convenient interface recombination phenomena at both homojunction and heterojunction, which lead to the saturation currents and ideality factors similar to those which are obtained by the present epitaxy techniques. It must be noted that the S hokley's law for heterojunction or homojunction (eqn. 6 and 7) can be easily changed to any other law as proposed in [11].

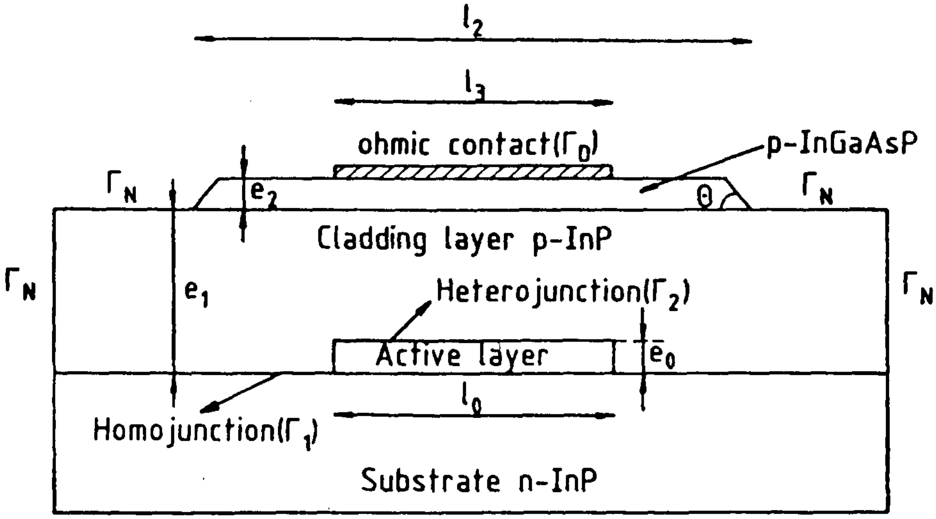

Figure 1 : Schematic view of a BRS laser

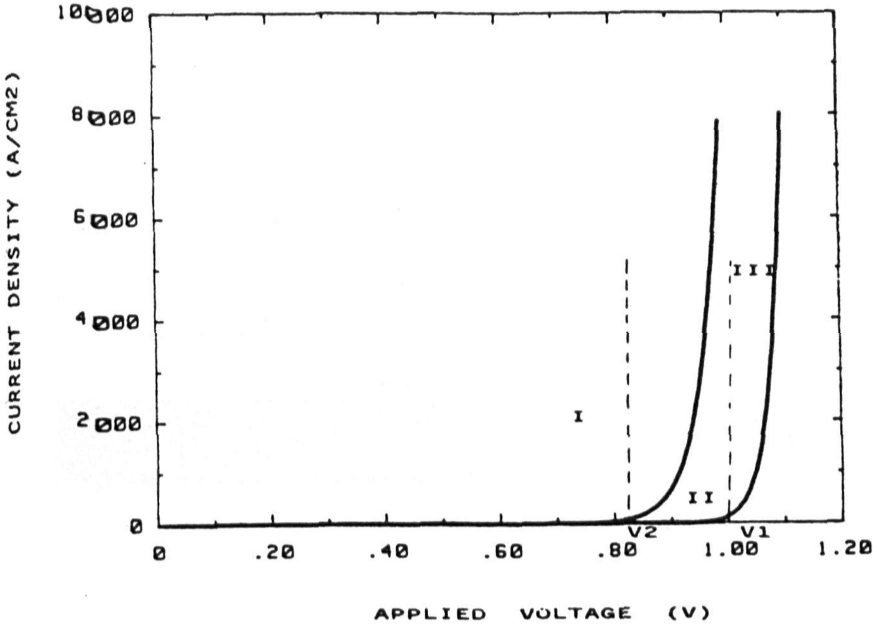

Figure 2 : Experimental current versus applied voltage characteristics for both homojunction and heterojunction.

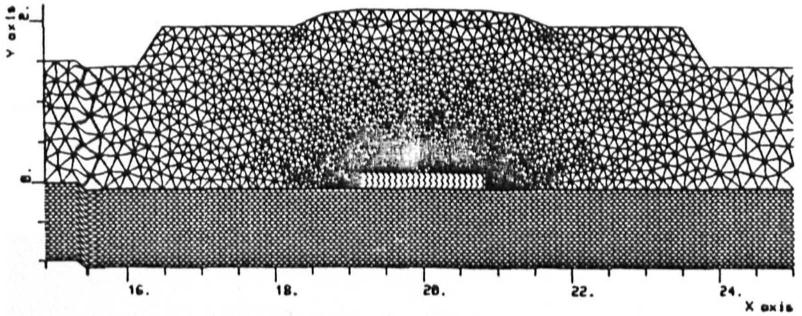

Figure 3 : Triangular mesh of the upper layer of a BRS laser using the TITAN III-V package.

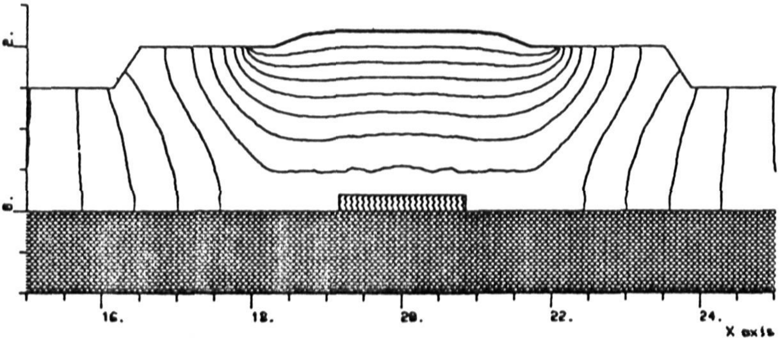

Figure 4 : Equipotential curves in a BRS laser (Applied voltage = 0.2 V)

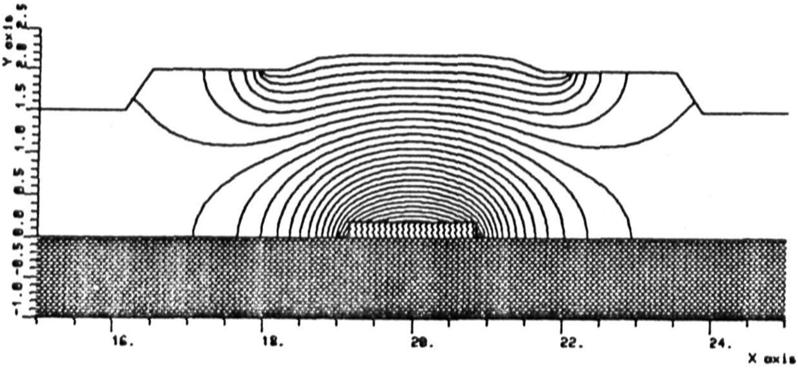

Figure 5 : Equipotential curves in a BRS laser (Applied voltage = 0.8 V)

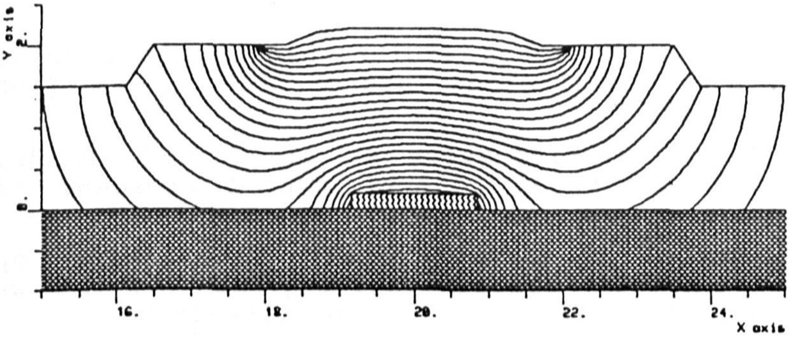

Figure 6 : Equipotential curves in a BRS laser
(Applied voltage = 1.2 V)

REFERENCES

[1]**K. Lau, A. Yariv** : "High frequency current modulation of semiconductor injection lasers", Semiconductors and Semimetals, Vol. 22, Academic Press (1985).

[2]**C. Su, V. Lanzisera** :"Ultra-high speed modulation of 1.3 μm InGaAsP diode lasers", IEEE QE-22, (1986), pp. 1568-1578.

[3]**V. Koren, G. Eisenstein et al.** " Wide Bandwidth modulation of three channel buried crescent laser diodes", El. Lett. 21, (1985), pp. 500-601.

[4]**K. Kamite, H. Sudo et al.** "Ultra-high speed InGaAsP/InP DFB lasers emitting at 1.3 μm wavelength", IEEE QE-23, (1987), pp. 1054-1058.

[5]**K. Souissi et al.**, submitted to COMPEL Journal, Dublin (1988).

[6]**E. Caquot et al.**, "Integration of process, device and circuit models for III-V devices", Lecture Notes of an I.S.C., Boole Press, Dublin, (June 1987), pp. 8-18.

[7]**P.L. George**, "MODULEF : Génération automatique de maillages", 2nd edition, INRIA editor (1986).

[8]**P.G. Ciarlet**, "Analyse Numérique Matricielle et optimisation", Masson, Paris (1982).

[9]**B.T. Polyac**, "The conjugate gradient method in extremal problems", U.S.S.R. Comp. Math. and Math. Phys., 9, (1969), pp. 94-112.

[10]**A. Paraskevopoulos**, Thèse de Docteur en Sciences, Université Paris XI, (1988).

[11]**S. Mottet et al.**, "Conduction mechanisms analysis and simulation of 1.3 μm laser diodes", Proc. of ESSDERC 87, Bologna, pp. 1003-1006.